Digital tender

Sensitivity Analysis of NTA8800 for a Dutch Building Renovation Tendering System

January 2021

DIGITAL TENDER

MMIP Line: 3.2

MMIP block: Industrialization & Digitization

BTIC Mainline & wp: WP4.2: Digitization of renovation process

Activity 2

Sensitivity Analysis of NTA8800 for a Dutch Building Renovation Tendering System

Table of Contents

Summary 1

1. Introduction 2

1.1 Background 2

1.2 Target: 2030 3

2. BTIC - MMIP - Integral Energy Transition Existing Construction 3

3. Problem description 4

4. Research Methodology 5

5. Sensitivity analysis and building energy performance 6

6. The under-investigation model 7

6.1 Model description 7

6.2 Model's input variables 7

7. Determining inputs of interest parameters and their variability 11

8. Selecting proper sensitivity analysis methods 15

8.1 Morris screening method 17

8.2 Sobol's method 20

9. Performing sensitivity analyses 22

9.1 Case study 22

9.2 Determining the minimum enough simulations for a robust result 23

9.3 Sensitivity analyses settings 25

10. Results and discussion 26

10.1 SA ranking results 26

10.2 Discussion 27

11. Conclusion 30

12. Acknowledgements 31

13. References 32

Summary

To achieve the national 2030 climate targets, we will have to rapidly increase the pace of renovation projects to over 50,000 existing homes per year by 2021. One of the barriers to achieving higher renovation rates is that most renovation activities are still at the craftsman stage [1], in which they are planned and implemented in separate approaches per dwelling. Given the mentioned energy-efficiency targets and deadlines set by EU countries, including the Netherlands, the housing renovation process needs a substantial upscaling. To this end, renovations' requirements need to be elicited in a structured format such that the building industry can offer standardized solutions that allow large scale, high-speed construction processes. These requirements should be incorporated in a publicly accessible digital platform enabling required data for heat transmission, CO2 emission, and construction cost calculations **to prepare the foundations for tendering renovation clusters allowing the construction companies to adapt their production process and achieve economies of scale.**

During this process, building energy simulation systems, especially those designed based on national-level regulations (e.g., NTA8800 in the Netherlands), play an essential role since they can calculate current building energy performance if the required information had been provided. Performing a holistic energy calculation requires two types of energy usage information. First, building-related energy consumption, which is related to the building's ability to avoid heat loss in winter and heat gain in summer and maximize natural light use. Second, user-related energy consumption, which is related to occupants' gas, electricity, and water consumption for cooking, domestic hot water, and electric equipment and appliances [2]. Although many of these inputs can be correlated based on their calculation methods, the required information must be aggregated from various data sources and seeking all of them simultaneously would be a burdensome and time-consuming task. When it comes to mass-scale renovation, the situation becomes even worse since data collection and information production must be handled not for a single house but thousands of dwellings. Thus, prioritizing input information is essential to facilitate and illuminate the orderly way of acquiring preliminary information.

This report's conducted study aims to **ascertain the prioritization of the most and least influential parameters for determining the total heating and cooling energy demand (BENG1) derived from NTA8800 regulations**. For that purpose, two well-known global sensitivity analysis methods, commonly used in the building energy performance simulations (Morris's and Sobol's methods), were selected and applied to the WoonConnect energy calculation software, which has been developed based on the NTA8800 regulations. Based on the literature, fifteen physical characteristics of a typical three-floor row dwelling were selected as the input factors for the sensitivity analyses. The analyses were performed with an adequate number of simulations to ensure results' robustness, which was further confirmed by attaining the same results from both applied methods. From the obtained results, the previously chosen input parameters were categorized into three priority levels. The top priority level gathers the parameters with a sensitivity measure greater than 0.05. The parameters in this category dramatically influence the heating and cooling energy demands, so providing this information has the top priority, and information must be as exact as possible. This priority level includes mostly dwellings' geometrical properties. The next priority was assigned to the parameters with sensitivity measures between 0.01 and 0.05, which moderately impacted the BENG1 value. However, since they

have mostly non-linear behavior, the uncertainty in information provision should be minimized as much as possible. All the parameters that reside in the second priority level directly relate to buildings' thermal properties. The last category encompasses all the other parameters with negligible effects on determining the BENG1 value. These parameters are mostly associated with the sun radiation part of energy demand calculations.

Within the following phase of the project, we will focus on providing information for required input parameters based on their priority level. Thus, in the next step, we will attempt to determine dwellings' geometrical properties from available data sources. Publicly available point clouds derived from aerial LiDAR surveys are valuable sources to extract dwellings required geometrical information. Because they are available countrywide, it is possible to use them in large-scale information extraction to accelerate dwellings' energy demand calculations and subsequently facilitate upscaling of the renovation process.

1. Introduction

1.1 Background

The building sector contributes significantly to world energy consumption. For instance, buildings in the EU are responsible for around 40% of the final energy consumption and 36% of CO2 emissions [3]. A considerable part of this energy consumption is attributed to the residential sector. On average, 27.2% of the total energy in the EU is consumed by dwellings [4]. Several reasons, including population growth, building services enhancement, remotely working occupations, and new lifestyles derived from global crises such as the recent pandemic, have increased the amount of time spent by individuals in dwellings. These shifts seem to indicate an upward trend in residential buildings' energy demand for the foreseeable future.

Fortunately, in recent years, significant progress has been made in producing energy-efficient and eco-friendly construction materials, most of which are incorporated in regulations to improve new buildings' energy performance [5]. Still, much of the high energy consumption problems are mainly attributed to existing buildings, of which many are aged more than 50 years [6] with relatively low energy efficiency. The Netherlands, for example, with more than 2.6 million houses built in the post-war period 1945-1975, has an overall average of 'D', on a scale from A to G, for dwellings' energy label performance [7].

Since nearly more than 80 percent of residential buildings were built before 1990 in Europe [6], renovating existing buildings would be a solution that can reduce the EU's total energy consumption and CO2 emissions by about 5% [1]. To fulfill the minimum energy performance according to Article 4 of Directive 2010/31/EU, an annual 3% rate of renovation of occupied buildings should be set by each EU member-state [8]. However, the current rate of the annual renovation of building stocks in the Netherlands is only 1.3% [9], less than half of the required rate and surprisingly not increasing per year [10]! Thus, the existing buildings' accelerating renovation rate is a core strategy for the EU [11] and also the Netherlands to meet its climate and energy objectives [5].

1.2 Target: 2030

To achieve the 2030 climate targets, we will have to rapidly increase the pace of renovation projects to over 50,000 existing homes per year by 2021. One of the barriers to achieving higher renovation rates is that most renovation activities are still at the craftsman stage [1], in which they are planned and implemented in separate approaches per dwelling. Given the above-mentioned energy-efficiency targets and deadlines set by EU countries, including the Netherlands, it is clear that the housing renovation process needs a substantial upscaling with industrial approaches to minimize waste, reduce costs, and optimize on-site productivity [1].

The existing challenges require novel approaches to address renovations at a different scale, larger than a single building but small enough to have common criteria for generating renovation solutions. This upscaling needs the contribution and integrity of technological and industrial knowledge, which must be applied to the current renovation process.

2. BTIC - MMIP - Integral Energy Transition Existing Construction

Within BTIC, consortia are initiated that consist of companies, government, and knowledge institutions and that jointly propose and implement innovation processes. It monitors the innovation processes' progress and gives its partners access to the knowledge and innovation developed. This leads to innovative technologies, processes, and social innovations. The objective of the BTIC program Integral energy transition for existing buildings, IEBB, is to have the (scientific and applied) research and innovation in the field of construction, design, and technology required to realize the objectives of the Climate Agreement.

Many fragmented and non-integrated processes occur in current construction and renovation practices. Within the IEBB project, this leads to the following solution. Through more cooperation and integration among the homeowners, suppliers, and government, end users can be offered a more integrated, cheaper, and less inconvenient renovation solution. Shortening process chains by digitization can save time and costs while at the same time increasing the profitability of the renovation sector. This insight is not new, but for the large-scale renovation tasks for the entire Dutch building

stock, breakthroughs will be necessary that go hand in hand with cultural changes with new forms of cooperation and alternative contracts. There are also opportunities to scale up tenders considerably by designing an innovative method of bundling the housing stock based on similar characteristics and similar renovation strategies. This opens the possibility of bundling the tenders. Various clients will have to work together in order to arrive at bundled tenders. For example, various housing associations, possibly together with homeowner corporations (Vereniging van Eigenaars – VvEs) and individual homeowners, can arrive at joint project definitions and tenders. Matching innovative business models must be further developed.

The BTIC program 'Integrated energy transition for existing buildings' (IEBB) consists of four sub-lines:

1. Renovation concepts
2. Sustainable individual heating systems
3. The transition process
4. Intelligent control of energy demand

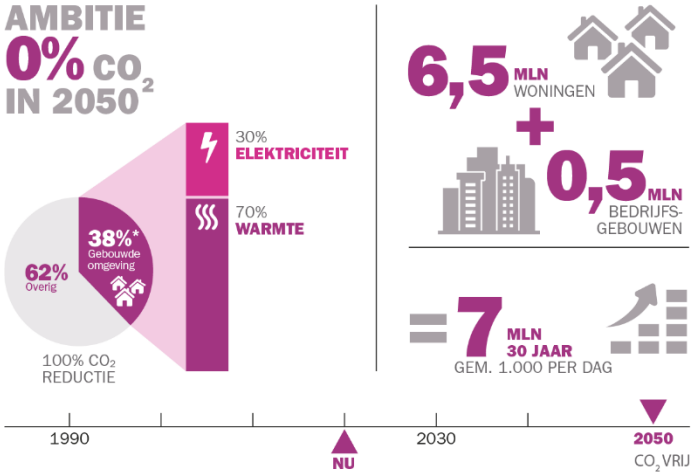

Figure 1- BTIC's ambition of housing renovation for a carbon-neutral environment

3. Problem description

During the process of mass-scale renovation, building energy simulation systems, especially those designed based on national-level regulations (e.g., NTA8800 in the Netherlands), play an important role since they can calculate current building energy performance if the required information is provided. Performing a holistic energy calculation requires two types of energy usage information. First, building-related energy consumption, which is related to the building's ability to avoid heat loss in winter and heat gain in summer and maximize natural light use. Second, user-related energy consumption, which is related to occupants' gas, electricity, and water consumption for cooking, domestic hot water, and electric equipment and appliances [2]. Although many of these inputs can be correlated based on their calculation methods, the required information must be aggregated from various data sources, which is a burdensome and time-consuming task. When it comes to mass-scale renovation, the situation becomes even worse since data collection and information production must be handled not for a single house but thousands of dwellings. Therefore, attempts at capturing data must be concentrated on the most determinative inputs (features for housing classification).

On the other hand, finding an optimal renovation solution in terms of energy performance requires a lot of effort. Since each of the dwellings has a specific optimized renovation solution, optimizing energy

performance includes numerous simulations considering different combinations of input parameters' values. However, identifying the most influential parameters of the simulation system can reduce the number of simulations and subsequent computational costs by focusing only on the most critical parameters. Thus, to generate the optimal renovation solution based on a specific building energy simulation system, it is crucial to know the extent of each input parameter's contribution to energy performance variation.

To handle the above-mentioned challenges, three questions must be answered.

- First: Among the required input parameters for building energy calculations based on NTA8800, which ones can be considered presumed fixed values without significantly affecting the output results?
- Second: Among the required input parameters for building energy calculations based on NTA8800, which parameters are in the top priorities for modifications to find optimal renovation solutions?
- Third: What are the available sources to collate information from for those parameters?

4. Research Methodology

As the literature suggests, sensitivity analysis is an excellent tool for prioritizing inputs based on their contribution to output variations. Thus, to adequately address the previous section's problem, sensitivity analyses were designed and implemented on NTA8800 input parameters of building envelope characteristics for the typical row-dwellings in the Netherlands. The WoonConnect energy calculation software developed by de Tweesnoeken was selected as the target model for these analyses since it has been developed based on NTA8800 regulation. Below, the following chapters of this document are briefly explained.

5. *Sensitivity analysis and building energy performance:*
   This section consists of an introduction to the concept of sensitivity analysis and its application in building energy performance modeling.
6. *Model description:*
   The model's architecture, its constituent, their relationship, and possible input variables have been explained in detail in this section.
7. *Determining inputs of interest parameters and their variability:*
   This section describes the process of selecting the sensitivity analyses input parameters based on the literature and NTA8800 requirements.
8. *Selecting proper sensitivity analysis methods:*
   From what has been extracted from the literature and similar previous efforts, this section indicates what kind of SA method would be more appropriate for under investigation model based on its characteristics and number of input parameters. Furthermore, in this section, the mathematical theory behind each of chosen methods has been elaborated.
9. *Performing sensitivity analyses:*
   This section describes the environment that has been built for conducting sensitivity analysis, the case study features, and how to set SA settings to achieve robust results.
10. *Results and discussion:*

In this section, the initial and in-depth results of the sensitivity analyses have been demonstrated and interpreted in details to justifying the drawn conclusion

11. *Conclusion:*
    This part will sum up the results that have been discussed in its previous section and present the conclusion derived from the analysis results.

5. Sensitivity analysis and building energy performance

Sensitivity analysis (SA) can be defined as *"the study of how uncertainty in the output of a numerical (or otherwise) model can be apportioned to different sources of uncertainty in the model input"* [12]. It is a systematic investigation by which assessors bridge the uncertainty gaps [13]. Such analysis is useful for the model's predictability and robustness. In other words, sensitivity analysis identifies priorities of the phenomenon under study [14] and is often employed to determine the importance of a model's input parameters on the behavior of the system [15].

The uses of sensitivity analysis can be of a wide range. However, these use cases can mainly be divided into four categories including decision making: to provide recommendations for decision-makers; communication: making recommendations more credible, understandable, compelling, or persuasive; increased understanding or quantification of the system; and model development: calibrating, simplifying, or testing the model for validity or accuracy [16].

Methods for performing sensitivity analysis are distinguished into two majors categories: local and global. Local (or differential) sensitivity analysis is based on one-factor-at-a-time methods in which one factor is changed while all the other ones are fixed [17]. A local SA measures a single parameter value's relative sensitivity to change in other parameters [15] around a point or base case. Despite its wide use due to its straightforwardness and low computational cost, local SA suffers from a lack of self-verification. This method's results are also limited around a base case, not the entire model [17]. Global SA methods, on the other hand, are more focused on the influences of uncertain inputs over the whole input space. It is a quantitative and rigorous overview of how different inputs influence the output. Given that some parameters play significant roles, while others are marginally important, make global SA a valuable tool and more reliable approach. However, they have a high computational cost and complexity, especially when the number of inputs is high [15].

Building energy performance analysis (BEPA) is an essential step towards having energy-efficient buildings in both design and renovation phases. Building energy performance models have been getting more and more complex throughout the years to enhance their accuracy and robustness. However, this complexity accompanying tries to have complete coverage of various input parameters makes it hard to measure the input parameters' overall influence on the output and identify their relative importance [18].

The SA capability to identify the most influential system's parameters and provide "if-then" analysis for decision support makes it a great solution for the above-mentioned problem. Thus, it has been widely used in several buildings' energy simulations thermal performance applications such as system calibration, Identification, optimization in design and operation, and buildings' renovation [6, 7].

6. The under-investigation model

6.1 Model description

The sensitivity analysis's target model is a software developed by de TweeSnoeken to calculate building energy performance based on NTA8800 regulations. This software is a part of a bigger platform of de TweeSnoeken company known as WoonConnect.

The mentioned software, currently running only on Windows operating system, has been coded in a .NET environment using C# programming language. The energy calculation part consists of two namespaces, one for the calculation part named Regelgeving.NTA8800 and the other for the input and output data are called Regelgeving.NTA8800Data.

The Regelgeving.NTA8800 namespace comprises of six folders including analysis, containing classes and methods to extract information from existing building models within the platform; Calculation, containing classes and methods to perform different energy calculations such as heating, cooling, ventilation, etc.; Formulas, contacting classes which have methods representing formulas from NTA8800 for energy calculations; Report, contacting report class for presenting the results; Tables, containing NTA8800 tables required for performing calculations.

The Regelgeving.NTA8800Data namespace includes input and output folders. The input folder contains the model input variables, defined in 32 classes associated with each other in 5 hierarchy levels, and the output folder includes classes storing values from performed calculations in the Calculation class as mentioned earlier. The output folder contains energy calculation results of building, lighting, heating and cooling, hot water, humidification, production, transmission, ventilation, and airflows.

6.2 Model's input variables

Each of the model's input classes represents different classifications of the building systems and elements contributing to the building's total energy consumption. The hierarchy and association within these classes are shown in Table 1. The associations between classes can be categorized into five different hierarchy levels, which are elaborated below.

Level 0 to Level 1:

NTA8800Building class, derived from Building class, contains general information of a building object considering NTA8800 definitions. Each NTA8800Building class is associated with at least one ClimateZone class (Figure 2).

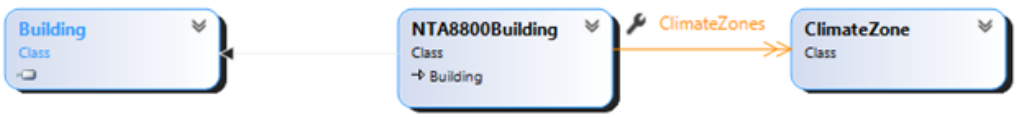

Figure 2- Object Diagram from level 0 to 1

Level 0 to Level 1:

ClimateZone class is referred to a part of a building that shared the same heating, ventilation, cooling, and hot water system. Most of the time, a typical residential building consists of only one climate zone. Apart from general information related to each climate zone, such as usage area and the number of

floors, a ClimateZone object contains one or more HotWaterSystem, and CalculationZone objects and zero or one object from each of the HeatingSystem, CoolingSystem, Ventilation, Humidification, and Production classes. All the associated classes with the ClimateZone, except the Ventilation class, are branched into more detailed classes (Figure 3).

Table 1- The hierarchy and association within the software classes

Level 0	Level 1	Level 2	Level 3	Level 4	Level 5
NTA8800 Building	Climate Zone	HotWater System	HotWaterShowerHeatRecoveryUnit		
			HotWaterSolarWaterHeater		
			HotWaterGeneration		
			HotWaterDistribution		
			HotWaterStorage		
		Heating System	HeatingStorage		
			HeatingGenerator		
			HeatingEmission		
			HeatingDistribution		
		Cooling System	CoolingGenerator		
			CoolingEmission		
			CoolingDistribution		
		Production	PvModule		
		Calculation Zone	VerticalConduit		
			UnheatedAdjacentRoom		
			UsageFunction		
			EnvelopePart	NTA8800Floor	
				NTA8800Window	
			LightingInOut	LightningZone	Lightning Daylight Segment
					Lightning Fixture

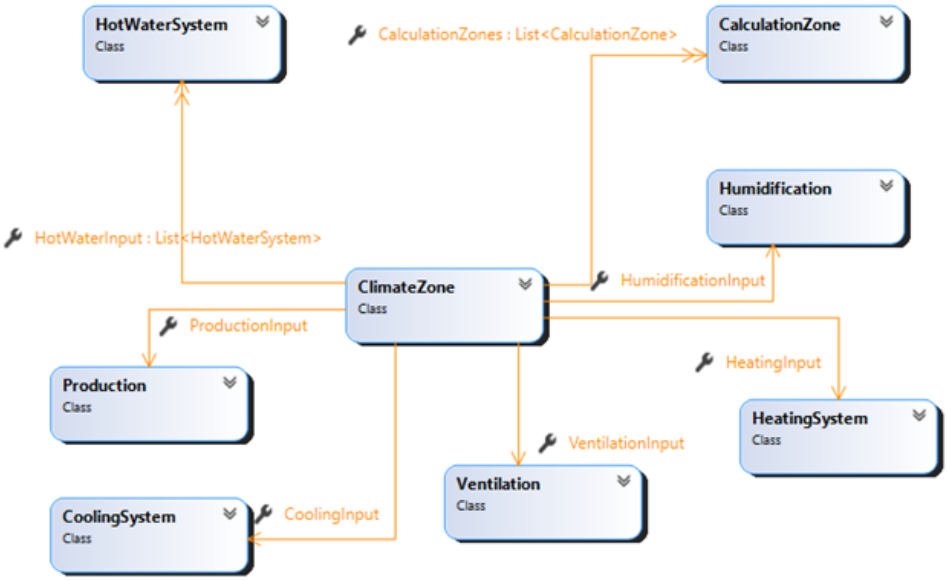

Figure 3- Object diagram for level 1 to 2

Level 2 to Level 3:

HotWaterSystem class contains properties about piping system towards kitchen and bathroom such as origin, length, and piping diameters. Other input information regarding the climate zones' hot water system such as generators, distribution, and storage systems is embedded into five classes branched from HotWaterSystem class, as shown in Figure 4.

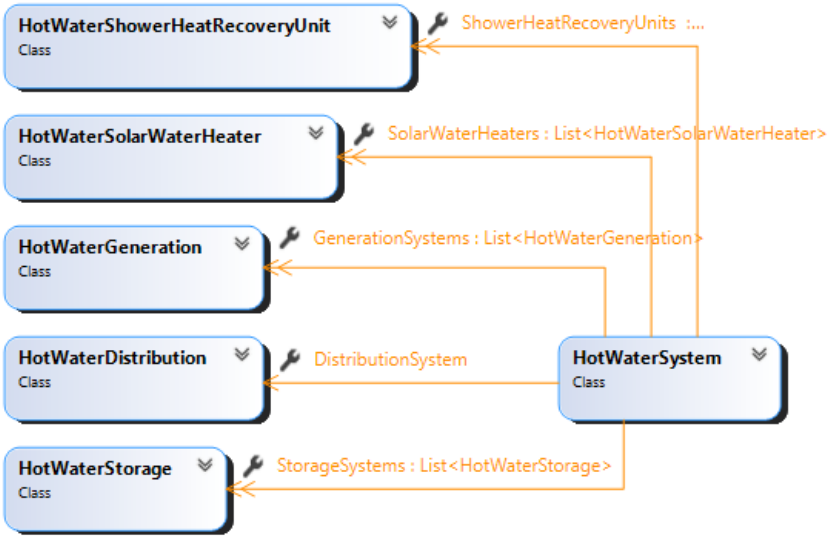

Figure 4- Hot water system object diagram

Other associated classes to the ClimateZone class (except ClaculationZone), including HeatingSystem, CoolingSystem, Production, and the classes branched from them, are shown in Figures 4 to 7.

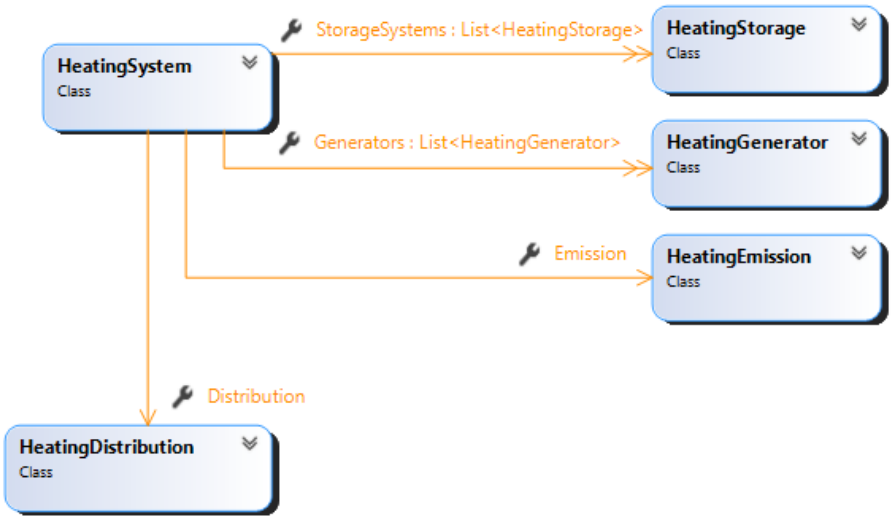

Figure 5- Heating system object diagram

CalculationZone class:

According to NTA8800 regulations, a calculation zone is a way of dividing buildings into logical units to perform energy calculations. Same as the climate zone, usually a typical house will consist of only one calculation zone. Many essential input variables for calculating building energy demands are included in CalculationZone class and its associated classes; input variables such as constructions mass, infiltration rate, building envelope properties, and lightning demand. Envelope parts properties are usually determining variables for both estimating energy demand and providing renovation solutions.

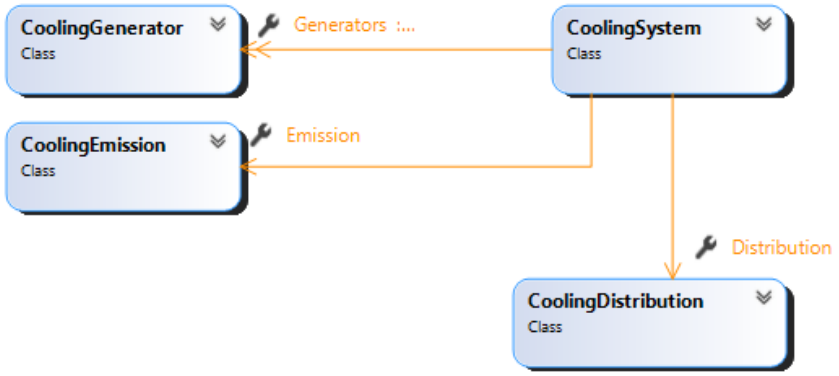

Figure 6- Cooling system object diagram

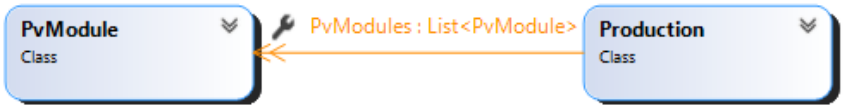

Figure 7- Production class object diagram

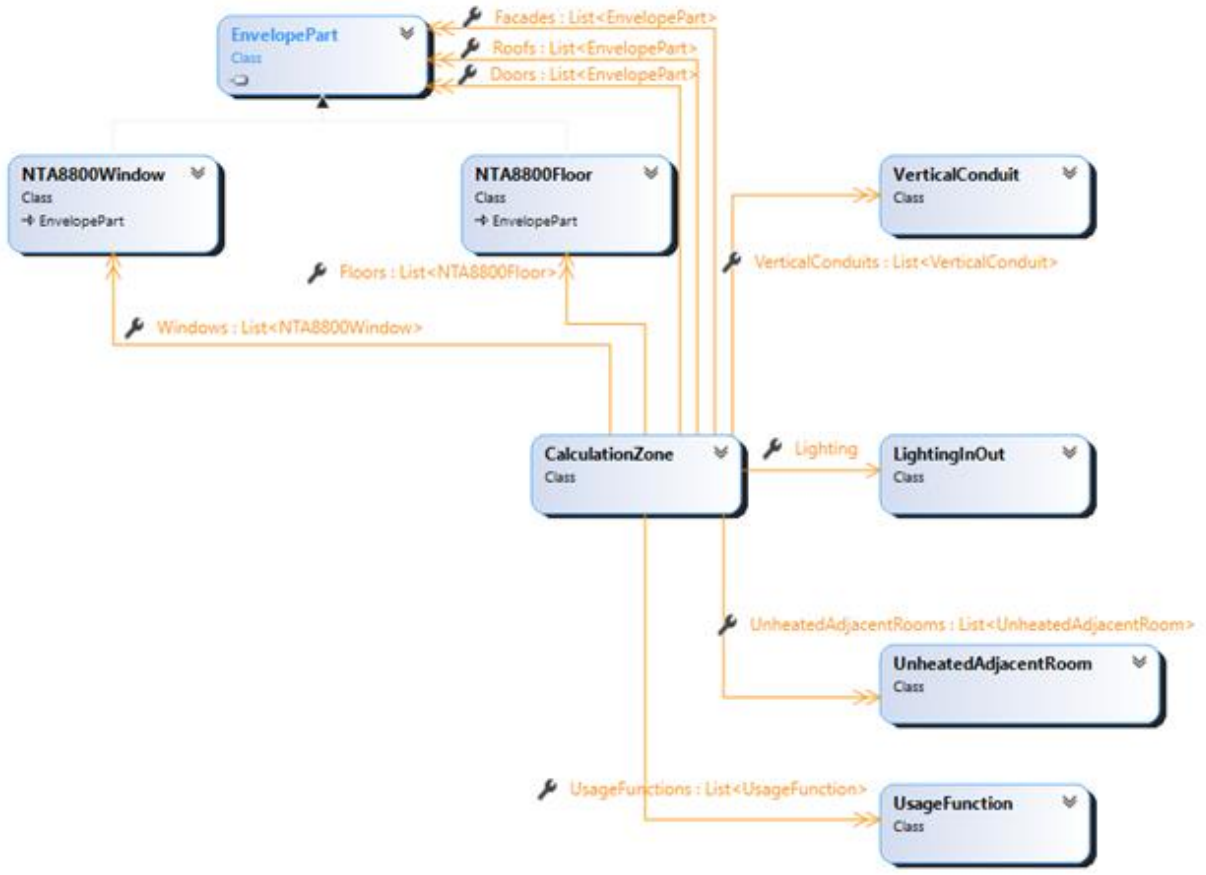

Figure 8- Calculation Zone object diagram

7. Determining inputs of interest parameters and their variability

A comprehensive literature review was conducted to find commonly used input factors and their variability range in the field of sensitivity analysis for energy demand estimation by building energy simulations. “Building,” “Energy Simulation,” and “Sensitivity Analysis” were used as keywords to search through the Scopus database with subject areas limited to “Engineering,” “Energy,” “Environmental Science,” and “Material Science”. As a result, 252 related English articles were found, each of which was manually investigated. Finally, only 21 articles directly related to our study subject (sensitivity analysis in energy demand/performance for building energy simulations of residential buildings) were found that specified the input variables, their variability range, and distribution functions for conducted sensitivity analyses. From these articles, all the input variables and their variability ranges were extracted and summarized in Table 2. Then these variables were compared to the ISO 52016-1 input data, NTA8800 specifications, and software input variables to identify the inputs of interest for carrying out the sensitivity analysis.

Table 2- Summary of input variables used for sensitivity analysis for building energy simulations extracted from reviewed articles

Parameter	ISO description	Unit	Distribution	Range	Reference
Geometry					

Area of each floor	Useful floor area per elementary space	m^2	Uniform	[0.5, 3]	[19], [20]
Orientation	Orientation angle per external building element (expressed as the geographical azimuth angle of the horizontal projection of the inclined surface normal; convention: angle from South, eastwards positive, westwards negative)	°	Uniform	[0, 360]	[21]
			Uniform	[0, 360]	[22]
			Uniform	[0, 360]	[19], [20]
			Uniform	[45, 135]	[23]
			Uniform	[0, 360]	[24]
			Uniform	[0, 180]	[25]
Window/Wall ratio	Glazed area, per window element		Uniform	[0.2, 0.8]	[21]
			Uniform	[0.1, 0.4]	[19], [20]
			Uniform	[0.05, 0.55]	[22]
			Uniform	[0.05, 0.65]	[23]
			Uniform	(0, 1)	[24]
			Uniform	(0, 0.6]	[26]
			Uniform	[0.1, 0.7]	[25]
External Wall and façade					
Rc	Thermal resistance, per opaque building element	$m^2.K/W$	Uniform	[1.12, 5.4]	[27]
			Uniform	[0.09, 1.85]	[22]
			Normal	4.7, 0.05*4.7	[28]
U-value	Thermal transmittance, per curtain wall	$W/m^2 \cdot K$	Triangle	0.11, 0.35, 1.5	[29]
			Uniform	[0.1, 0.5]	[21]
			Uniform	[0.2, 0.4]	[30]
			Uniform	[0.3, 1.5]	[31]
			Discrete-Uniform	[0.75, 1.75, 2.75, 3.75]	[32], [33]
			Uniform	[0.4, 3.85]	[34]
			Uniform	[0.3, 0.6]	[35]
Window					
U-value	Thermal transmittance, per window	$W/m^2 \cdot K$	Uniform	[1.1, 2.5]	[36]
			Triangle	0.9, 1.78, 3.1	[29]
			Uniform	[1, 3]	[21]
			Uniform	[1, 3]	[30]
			Normal	1.1,0.11	[37]
			Uniform	[0.5, 6]	[22]
			Uniform	[1.5, 6.5]	[31]
			Normal	1.1, 0.004*1.1	[28]
			Uniform	[0.6, 4.6]	[25]
			Uniform	[0.9, 3.2]	[23]
			Uniform	[2, 4]	[38]
			Uniform	[0.85, 5.75]	[34]
Solar Heat Gain Coefficient [G value]	Total solar energy transmittance at normal incidence, for the transparent part, per transparent building element with non-scattering glazing	-	Triangle	[0.5, 0.7, 0.85]	[29]
			Uniform	[0.3, 0.7]	[21]
			Uniform	[0.2, 0.8]	[30]
			Uniform	[0.2, 0.9]	[22]
			Uniform	[0.3, 0.7]	[31]
			Normal	0.7, 0.006*0.7	[28]

			Uniform	[0.36, 0.53, 0.7, 0.87]	[32], [33]
			Uniform	[0.1, 0.9]	[25]
			Discrete-Uniform	[0.2, 0.4, 0.6, 0.8]	[39]
			Uniform	[0.22, 0.76]	[23]
			Uniform	(0,1)	[24]
			Uniform	[0.2, 0.5]	[35]
			Uniform	[0.2, 0.6]	[34]
Overhang depth	Depth of a (simple) overhang (or similar shading object)	m	Uniform	[0, 2]	[23]
			Uniform	[0, 0.5]	[24]
			Uniform	[0.1, 1]	[36]
Overhang projection factor		m	Uniform	[0.1, 1.5]	[22]
			Uniform	[0, 0.42]	[34]
Overhang height	Height, per shaded surface, from bottom to top; if tilted: vertical projection	m	Uniform	[0, 0.5]	[23]
Floor and Ceiling					
U-value	Thermal transmittance, per opaque element	$W/m^2 \cdot K$	Triangle	[0.15, 0.62, 2]	[29]
			Discrete-Uniform	[0.8, 1.9, 3, 4.1]	[32], [33]
			Uniform	[0.1, 1.1]	[25]
Rc	Thermal resistance, per opaque building element	$m^2.K/W$	Normal	5, 0.05*5	[28]
Roof					
U-value	Thermal transmittance, per opaque element	$W/m^2 \cdot K$	Triangle	[0.09, 0.29, 1]	[29]
			Uniform	[0.1, 0.4]	[21]
			Uniform	[0.1, 0.3]	[30]
			Discrete-Uniform	[0.8, 1.9, 3, 4.1]	[32], [33]
			Uniform	[0.2, 0.4]	[38]
			Uniform	[0.1,0.9]	[25]
Rc	Thermal resistance, per opaque building element	$m^2.K/W$	Normal	5, 0.05*5	[28]
			Uniform	[0.2, 0.8]	[39]
Other					
Infiltration rate	Monthly time-average airflow rate of airflow element, k entering the thermal zone, for heating/cooling, for each month	dm^3/m^2s	Uniform	[0.01, 0.22]	[36]
			Normal	0.5, 0.2*0.5	[19], [20]
			Uniform	[0.6, 0.8]	[35]
			Uniform	[0.5, 1.5]	[25]

According to NTA8800, the valid range of window solar heat coefficient (G-value) is between the minimum value of 0.4 for a glazing type of “triple glass with two spectral selective and low emissive coatings” and a maximum value of 0.85 for a “one glass window”. However, in the presence of sun blinds, this range will multiply to the solar heat gain reduction factor (F_c) varying from 0.12 to 0.9 depending on the type, color, and control type of sun blinds and window orientation. Also, for

considering the impact of frame fraction, a range of 15 to 25 percentage of window area was assigned for its variability.

Each of the reviewed studies in Table 2 considers different shading properties (depth, height, and projection factor of the overhang) in their analysis. NTA8800 regulation employs heating and cooling shade reduction factors based on an obstruction's relative height (h_b), the relative width of an obstruction (b_b), the relative height of an overhang (h_o), window orientation, window inclination, and the year's months. Depending on the obstruction situation, a total of 14 different combinations, shown in Table 3, must be used to determine the shade reduction factor.

The infiltration rate or qv10 in NTA8800 is highly dependent on the building type, position, number of layers, roof type, and construction year and varies from $0.35\ dm^3/m^2s\ to\ 4.2\ dm^3/m^2s$. However, for our case study, a row dwelling with a middle position, this range will be shrunk to $0.7\ dm^3/m^2s\ to\ 3\ dm^3/m^2s$. In addition to the parameters mentioned above, for needed energy estimation, the software considers the specific internal heat capacity based on the mass of the construction per square meter of usable surface and type of ceiling (open or closed), which leads to 6 different combinations with 7 different outputs as shown in Table 4.

Based on the literature, the BENG value also depends on the building compactness, whose value is equal to the ratio between the building envelope's surface area (Als) and the heated floor area (Ag). Therefore, to evaluate the compactness influence relative to other input factors, it was decided to include the Als/Ag as one of the sensitivity analysis input parameters with a variability range between 1.2 to 1.9. The method of its implementation will be discussed in more detail in Section 9.

Considering what has been explained above, 15 variables were finally chosen as input parameters for conducting sensitivity analysis on the energy calculation software. These variables, their variability ranges, and distributions can be found in Table 5.

Table 3- Different scenarios for window obstruction extracted from NTA8800

	$h_b\ (m)$	$b_b\ (m)$	$h_o\ (m)$	Number of combinations
Minimal obstruction	$0. \leq 36$	≥ 3.73	≥ 1	1
Parallel obstruction	$(0.36, 0.5)$	≥ 3.73	≥ 1	3
	$[0.5, 1)$			
	≥ 1			
Flat overhang	≤ 0.36	≥ 3.73	< 0.5	3
			$[0.5, 1)$	
			≥ 1	
Left-side barrier	≤ 0.36	< 1	≥ 1	2
		≥ 1		
Right-side barrier	≤ 0.36	< 1	≥ 1	2
		≥ 1		
Both-side barrier	≤ 0.36	< 1	≥ 1	2
		≥ 1		
Complete obstruction	≥ 0.36		< 1	1

Table 4- Value of Specific internal heat capacity from NTA8800

Mass of construction (kg/m^2)	Specific internal heat capacity (k$J/m^2.K$)	
	Closed ceiling	Open ceiling
Less than 250	55	80
Between 250 to 500	110	180
Between 500 to 750	180	360
More than 750	250	450

Table 5- Chosen set of variables and their variability characteristics to use as input factors for sensitivity analyses

Input parameter	**Range**	**Unit**	**Variable type**	**Distribution**
Roof Rc	[0.5, 6]	$m^2.K/W$	Continuous	Uniform
Floor Rc	[0.5, 6]	$m^2.K/W$	Continuous	Uniform
Facades Rc	[0.5, 6]	$m^2.K/W$	Continuous	Uniform
Windows to wall ratio	[0.1, 0.7]	-	Continuous	Uniform
Windows U-value	[1.2, 4.5]	$W/m^2 \cdot K$	Continuous	Uniform
Windows G-value	[0.4, 0.85]	$W/m^2 \cdot K$	Continuous	Uniform
Windows frame fraction	[0.15, 0.3]	-	Continuous	Uniform
Windows obstruction scenario	[1, 2, 3, 4, 5, 6, 7, 8, 9, 10, 11, 12, 13, 14]	-	Discrete	Uniform
Windows sunblind type	[1, 2, 3, 4, 5]	-	Discrete	Uniform
Windows sunblind colour	[1, 2, 3]	-	Discrete	Uniform
Windows sunblind control type	[1, 2, 3]	-	Discrete	Uniform
Als/Ag	(1.1, 1.9]	m^2	Continuous	Uniform
Infiltration rate	[0.7, 3]	dm^3/m^2s	Continuous	Uniform
Specific internal heat capacity	[55, 80, 110, 180, 250, 360, 450]	$kJ/m^2.K$	Discrete	Uniform
Orientation	[0, 45, 90, 75, 180]	°	Discrete	Uniform

8. Selecting proper sensitivity analysis methods

Based on the literature [6, 7, 10, 11, 12], four main criteria, including system linearity, system monotonicity, the importance of the computational efficiency, and the number of inputs, were considered to select sensitivity analysis methods.

System linearity: Non-linear. Although many energy calculation functions are linear at first glance, NTA8800 regulation relies on various pre-defined tables. Different values are picked based on certain conditions, which can increase the whole system's non-linearity.

System monotonicity: Not monotonic. Increasing some inputs can result in a decrease in the energy needs and use (e.g., thermal resistance), while some inputs may have an inverse relationship with the energy performance (e.g., solar heat gain coefficient and heat generator efficiency).

Importance of computational efficiency: Low. Fortunately, the simulation system can generate outputs at a decent speed (0.02 sec/one simulation), so computational cost, in this case, was not an issue to consider.

The number of inputs: Low. As previously described, 15 variables have been chosen as input parameters for sensitivity analysis, which is relevantly low considering the simulation speed.

Iooss and Lemaire presented a chart in which different SA methods are positioned based on the target model's conditions, computational cost, and the type of information presented by each method [40]. Pang et al., based on Pianosi et al.'s work [42], added robustness to that chart and drew it similar to what is shown in Figure 9 [18]. The orange rectangle illustrated in Figure 9 shows the suitable options for performing SA in our case since the target model is complex, but there is no significant computational cost limitation.

To narrow down the choices and find appropriate SA methods, Rocuigny et al. presented a decision diagram (Figure 10) based on the model's linearity, monotonicity, and the number of input candidates contributing to sensitivity analysis [41]. Based on this flowchart, variance-based methods such as Sobol and FAST, as well as the Morris screening method, are the appropriate choices for our understudy case. The orange rectangle shows the area in which our model's condition fits.

As the literature suggests, in case multiple options are available, conducting at least two appropriate SA methods can reinforce the general conclusions drawn from analyses. Morris screening method, coupled with a variance-based method, is a common approach in many scientific fields. In this regard, both Sobol variance-based and the Morris screening Method were selected as the target sensitivity analysis methods for the under investigation energy calculation model.

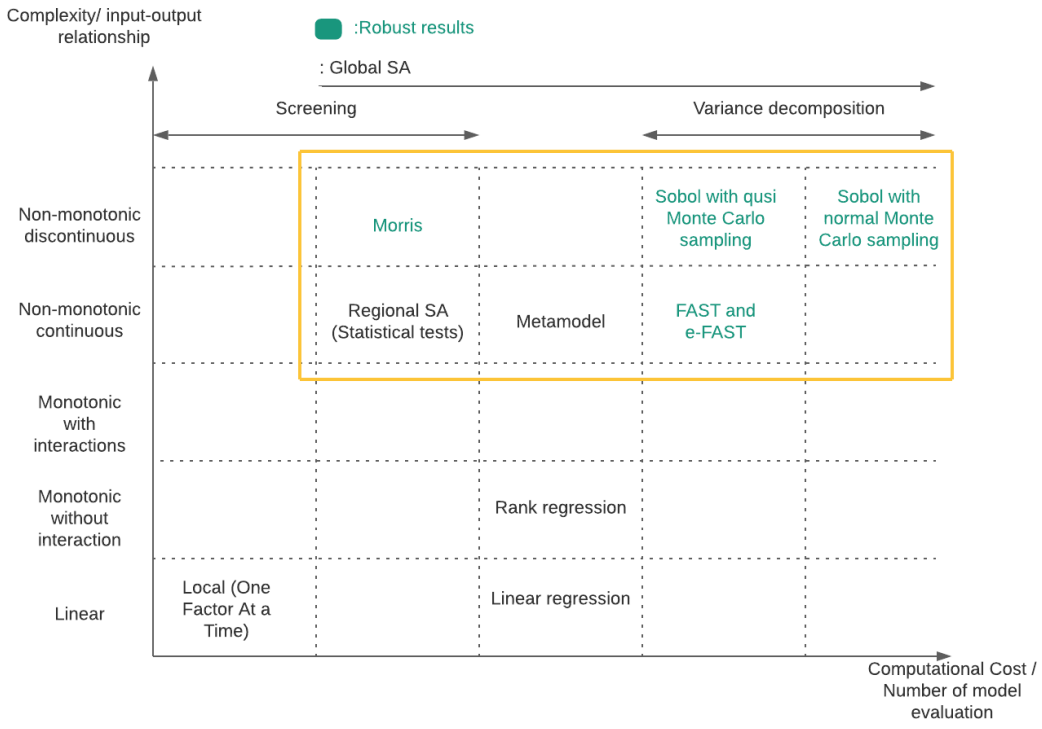

Figure 9-A positioning chart for different SA methods based on model characteristics presented by Pang et al.

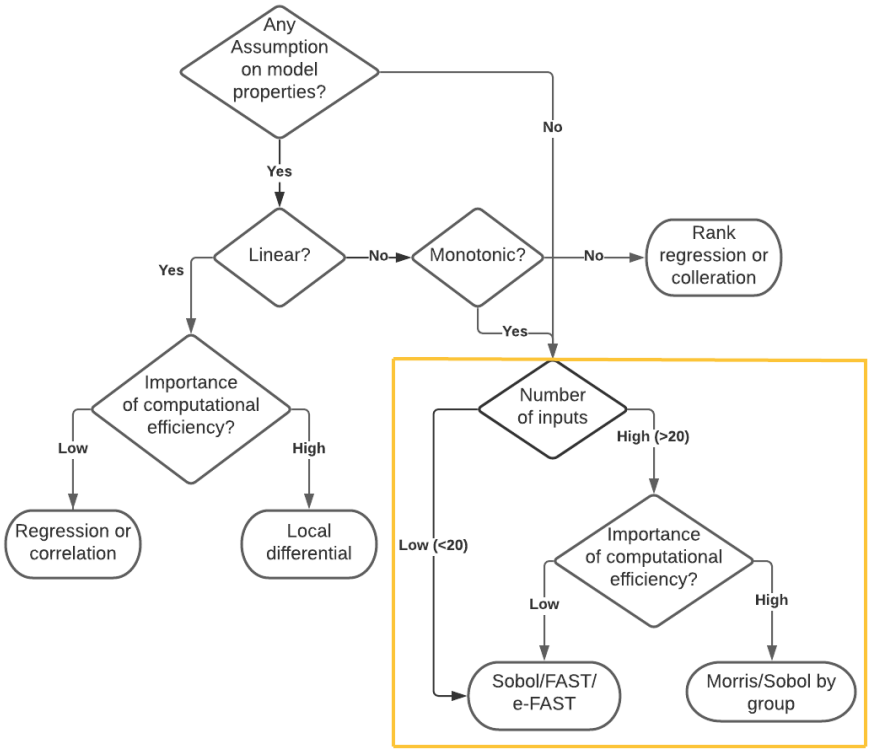

Figure 10- Decision diagram for selecting proper SA method [41]

8.1 Morris screening method

Screening methods rank the importance of the model parameters using a relatively small number of model executions. However, they tend to give qualitative measures. Meaningful information resides in the rank itself but not in the exact importance of the output parameters. These methods are precious to identify the non-influential parameters of a model, which could be safely excluded from further detailed analysis. This exclusion step is important to reduce the problem's size, especially if a more expensive method is to be applied at the next step. In this work, attention was paid to a particular screening method proposed by Morris [43].

The Morris or Elementary Effect Test method [16] is a screening method relying on an extension of the local sensitivity analysis OAT (One-Factor-At-a-Time) concept, i.e., two successive points differ only by one factor [44]. Morris's method determines which input factors have negligible effects, large linear effects without interactions, and large non-linear and/or interaction effects [40]. What follows, first describe the Local OAT method, then the method of Morris based on it.

Suppose X is a vector of input parameters for sensitivity analysis $x_1, \dots, x_k$ as shown in Eq. (1). In the OAT approach, first, the base vector $\bar{X}$, based on a real case or randomly, is defined by assigning $\bar{x}_1, \dots, \bar{x}_k$ values to correspondent $x_1, \dots, x_k$ input parameters Eq. (2). Then the sensitivity measure for the i-th input ($\hat{S}_i(\bar{X})$) takes from Eq. (3) where g is the function that maps the input factors into the output, Δ_i is the value of the deviation of i-th input from its base vector value, and c_i is the scaling factor.

$$X = [x_1, \dots, x_k] \quad (1)$$

$$\bar{X} = [x_1 = \bar{x}_1, \dots, x_k = \bar{x}_k] \quad (2)$$

$$\hat{S}_i(\bar{X}) = \frac{g(\bar{x}_1,\dots,\bar{x}_i+\Delta_i,\dots,\bar{x}_k)-g(\bar{x}_1,\dots,\bar{x}_i,\dots,\bar{x}_k)}{\Delta_i} c_i \quad (3)$$

However, Morris's method's approach is to compute output variations from multiple base input vectors within the feasible input space and to calculate the global sensitivity by summing up the value of these individual sensitivities [42]. The SA measures derived from Morris's method are based on calculating the elementary effects' statistical measures. An improved version of Morris's method proposed by G. Pujol has been employed in this report. The characteristics of the employed method have described below [44]:

Factor:

For the given input vector X $(\text{Eq. } (1))$, the input variables $x_1 \dots x_k$ are called factors.

Trajectory:

For the given input vector X with k factors, each trajectory consists of $k+1$ k-dimension vectors; each consists of k values within corresponding factors' variability space. The total number of trajectories, r, is defined by the user. r should be large enough to compute statistics such as mean and standard deviations [44].

Starting point:

Each trajectory has one starting point (base vector), $\bar{X}_0$, which is randomly chosen on the grid. Eq. (4) shows the starting point of the jth trajectory.

$$\bar{X}_0^j = [\bar{x}^j{}_1, \dots, \bar{x}^j{}_k] \qquad (j = 1, \dots, r) \quad (4)$$

Sample points:

Each trajectory consists of k sample points generated from the trajectory's starting point based on Eq. (5) [44].

$$\bar{X}_i^j = \bar{X}_{i-1}^j + \Delta_i e_i \qquad (j = 1, \dots, r \; and \; i = 1, \dots, k) \quad (5)$$

In Eq. 5, Δ_i is a multiple of the grid spacing in the ith direction, and e is a vector of zeros except for the ith factor (Eq. (6)).

$$\Delta_i e_i = [0, \dots, 0, \Delta_i, \dots, 0] \quad (6)$$

Elementary effect:

The elementary effect of the i-th factor in the j-th trajectory (EE_i^j) is defined as Eq. (7) [44]:

$$EE_i^j = \frac{g\left(\bar{X}_i^j\right) - g\left(\bar{X}_{i-1}^j\right)}{\Delta} \quad (7)$$

In Eq. (5) and (6), Δ_i is the step value for changing the value of x_i within its acceptable variation range Figure 11.

$$if\ a, h\ \in R, \forall\ x_i\ \in [a, h] \rightarrow\ \Delta_i = \Delta \times (h - a) \quad (8)$$

Δ, the grid jump determines the magnitude of steps. The convenient choice Δ is shown in Eq. (9), where p (must be even) is the number of levels chosen by the user [45].

$$\Delta = p/[2(p-1)] \quad (9)$$

p or the number of levels determines the grid size, which for each factor is equal to $1/(p-1)$ of the range of the factor's variability [42]. In other words, the variation range of the ith factor, x_i, is divided to $(p-1)$ equally sized sections Figure 11. The typical values for p ranges from 4 to 8 ($2/3 \leq \Delta \leq 4/7$) since these setups, allow elementary effects to capture finite and rather large perturbations [42].

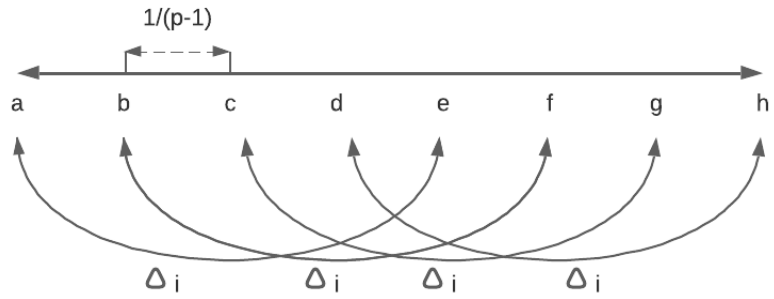

Figure 11 – Grid size and Δ_i in a supposed variability range of $[a, h]$ given p = 8

Trajectories' starting points are randomly generated over a uniform grid of the subsequent p points (e.g., $[a, b, c, d, e, f, g, h]$ in Figure 11) by moving one factor at a time of a fixed amount of Δ_i [42].

The sensitivity indexes derived from the method of Morris are comprised of μ, μ^* and σ [34]. The statistical summary of EE_i from the sampled trajectories can be achieved by calculating μ_i (Eq. (10)). μ_i is the elementary effects' mean value for the i-th input variable, which enables measuring the variable's influence concerning its direct or inverse relationship to output variation. As a change in a parameter value might have a changing sign on the output and thus result in a cancelation effect (as can be the case for a nonmonotonic function) Campolongo et al. [46] proposed the use of the mean of the absolute elementary effects, μ_i^* (Eq. (11)), to circumvent this issue. σ_i (Eq. (12)) is the standard deviation of the i-th input's elementary effects over all the trajectories, which estimates the ensemble of the input's higher-order effects, i.e., the interaction with other inputs and/or the non-linearity effect. Given r trajectories, the sensitivity indexes of the Morris method for the i-th element are calculated as follows:

$$\mu_i = \frac{1}{r}\sum_{j=1}^{r} EE_i^j \quad (10)$$

$$\mu_i^* = \frac{1}{r}\sum_{j=1}^{r}\left|EE_i^j\right| \quad (11)$$

$$\sigma_i = \sqrt{\frac{1}{(r-1)}\sum_{j=1}^{r}(EE_i^j - \mu_i)^2} \quad (12)$$

Besides, the ratio between standard deviation and absolute average can be used as a measure of non-linearity effect for each parameter or interactions with other inputs [34]. Concerning different ranges of σ_i/μ_i^*, input variables are considered as almost linear ($\sigma_i/\mu_i^* < 0.1$), monotonic ($0.1 \leq \sigma_i/\mu_i^* < 0.5$), almost monotonic ($0.5 \leq \sigma_i/\mu_i^* < 1$), or non-monotonic and nonlinear ($\sigma_i/\mu_i^* \geq 1$) [34].

Thus, there are three possible categories of parameter importance:

1. Parameters with non-influential effects, i.e., the parameters that have relatively small values of both μ^* and σ. The small values of both indicate that the parameter has a negligible overall effect on the model output.
2. Parameters with linear and/or additive effects, i.e., the parameters that have a relatively large value of μ^* and relatively small value of σ. This indicates that the variation of elementary effects is small, while the magnitude of the effect itself is consistently large for the parameter space's perturbations.
3. Parameters with nonlinear and/or interaction effects, i.e., the parameters with a relatively moderate value of μ^* and a relatively large value of σ. A large value of σ indicates that the effect's variation is considerable; the effect can be large or negligibly small depending on the other values of parameters at which the model is evaluated. Such large variation is a symptom of nonlinear effects and/or parameter interaction.

The computational cost for the Morris method (number of simulation runs) is equal to $r(k+1)$ model evaluations, in which r is the number of trajectories defined by the user and k is the number of input factors. This method's computational cost is far less than other sensitivity analysis methods since setting the r value around 10 is usually enough to reach a convergence [47][42][18].

8.2 Sobol's method

Another method used in this work is the Sobol variance-based SA method, in which the output's uncertainty is decomposed into a sum of corresponding inputs' variance and the combinations thereof [17] [18]. The variance-based method includes three basic principles [42]:

1. Input factors are considered as stochastic variables so that the model induces a distribution in the output space
2. The variance of the output distribution is a good proxy of output uncertainty
3. The contribution to the output variance from a given input factor is a measure of sensitivity

Assume that the model under investigation is described as a square-integrable function $f: X \in [0,1]^D \mapsto Y = f(X) \in R$, where Y is a scalar output, and X is a set of k input factors $(x_1, \dots, x_k)$, which are supposed to be random variables described by known probability distributions with variability ranges scaled over 0 to 1. The high dimensional model representation (HDMR) of $f(X)$ is a linear combination of functions with increasing dimensionality as it is shown in Eq. (13), where f_0 is a constant [48].

$$f(X) = f_0 + \sum_{i=1}^{k} f_i(x_j) + \sum_{1\leq i<j}^{k} f_{ij}(x_i, x_j) + \cdots + f_{1,\dots,k}(x_1, \dots, x_k) \quad (13)$$

Moreover, if the input factors are mutually independent, a functional decomposition of the variance, also known as functional ANOVA (Analysis of Variance), is available as it is shown in Eq. (14) [49]:

$$V(Y) = \sum_{i=1}^{k} V_i + \sum_{1 \le i < j}^{k} V_{ij} + \cdots + V_{1,\ldots,k} \quad (14)$$

Where V_i, V_{ij}, $V_{1,\ldots,k}$ denote the variance of f_i, f_{ij}, $f_{1,\ldots,k}$ respectivezly:

$V_i = V\left(E(Y|X_i)\right)$

$V_{ij} = V\left(E(Y|X_i, X_j)\right) - V_i - V_j$

$V_{ijk} = V\left(E(Y|X_i, X_j, X_k)\right) - V_{ij} - V_{ik} - V_{jk} - V_i - V_j - V_k$

.

.

.

$$V_{1,\ldots,k} = V(Y) - \sum_{i=1}^{k} V_i - \sum_{1 \le i < j}^{k} V_{ij} + \cdots + \sum_{1 \le i < j}^{k-1} V_{1,\ldots,k-1} \quad (15)$$

Then a normalized variance-based sensitivity measure for the first-order effect of a model input parameter X_i can be written as:

$$S_i = \frac{V_i}{V(Y)} \quad (16)$$

The first-order SA index, also known as “the main effect”, measures the direct contribution to the output variance from individual input factors or, in other words, the expected reduction in output variance that can be obtained by assigning a fixed value to a specific input [42]. The other terms of the decomposition can similarly be interpreted as higher-order sensitivity indexes [50].

$$S_{ij} = \frac{V_{ij}}{V(Y)}, S_{ijz} = \frac{V_{ijz}}{V(Y)} \quad (17)$$

Homma and Saltelli [51] introduced an additional index, the total-order sensitivity index, S_{Ti}, that accounts for all the contributions to the output variation due to factor x_i (i.e., first-order index plus all its interactions):

$$S_{Ti} = S_i + \sum_{j \ne i} S_{ij} + \cdots + S_{1,\ldots,k} \quad (18)$$

Thus, $S_i \le S_{Ti} \le 1$

Based on the sensitivity analysis's objective, each of the first order and total order sensitivity indices has different applications. For instance, to fix the factors which are not important (determining negligible factors) in the energy models, the total sensitivity index should be used. On the other hand, if the purpose is prioritizing energy-saving measures, the first-order effects would be a better option [17].

Sampling method for Sobol sensitivity analysis:

The Sobol sequence, a quasi-random sequence, is the most suitable for the computation of the variance-based SA indices. A quasi-random sequence is a set of sampling techniques used to improve the normal Monte Carlo simulation's convergence rate. In these methods, each sample point is generated regarding previous ones, which dramatically prevents clusters' occurrence [18]. In this work, an improved scheme for the Sobol sequence sampling method proposed by Saltelli has been used. This scheme for calculating all effects of the first and total order requires $n(k+2)$ simulations and $2n(k+$

2) for calculating second order effects as well. In the recent formulas, k is the number of input factors, and n represents coefficient, which varies depending on the requirement for the accuracy of the result. The value of n is usually around 1000 or more, depending on the case and required confidence intervals [18].

9. Performing sensitivity analyses

For conducting sensitivity analysis, an integrated environment was built by scripting in Python programming language and creating test functions in the software source code within Visual Studio environment using C# language programming and .NET framework. Within the environment, the information exchange was enabled through CSV files and Microsoft.Data.Analysis (version 4.0) NuGet package. This package brings the option of working with data frames, as does the Pandas library for Python (Figure 12). For generating samples and conducting analyses, the SALib library was used. SALib is an open-source Python library of commonly used sensitivity analysis methods, including Sobol, Morris, and FAST [52].

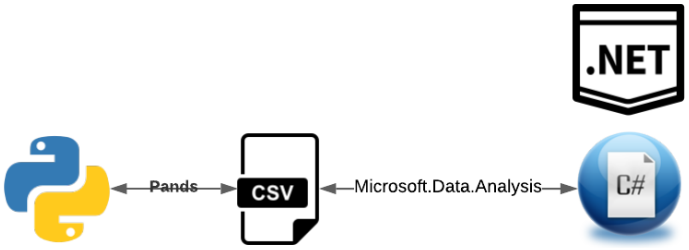

Figure 12- Information exchange between Python and .Net environment

9.1 Case study

A typical row dwelling in the middle position with two façades in front and back with windows in each and two adiabatic sidewalls was considered a case study. The input factors for the sensitivity analyses correspond to what has previously been described in section 7, Table 5.

In this study, the under-investigation row dwelling consists of a total of 3 floors, one of which is the attic. For implementing the building compactness (the ratio between the surface area of the building envelope and the heated floor area), we extend only the building's length since it is an independent dimension from window to wall ratio, which is the other geometrical input variable in our sensitivity analysis. The dimension settings for the row dwelling as a sensitivity analysis model are described in

Figure 13. All of the building dimensions are fixed except for the building length to generate different buildings with different compactness values.

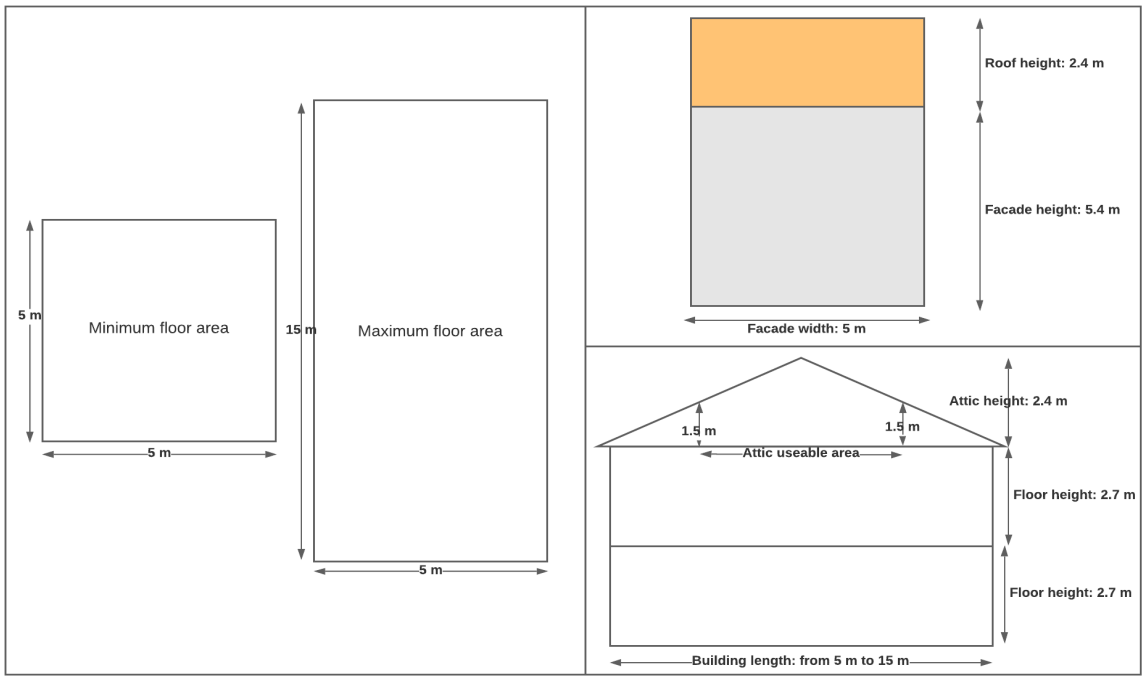

Figure 13 - The case study and its geometrical variability to enable compactness (Als/Ag) as one of the input variables for sensitivity analysis. Left: Floor plan view, the minimum and maximum range for floor area variation, Top right: Façade view, the façade and roof dimensions, bottom right: Cross-section view, the useable attic area, and building height dimensions.

The ratio of area loss to the heated area can be calculated as Eq. (19) where Fl_A is the area of each floor, Fc_A is the façade area, R_A is the roof area and A_{UA} is equal to the useable area of the attic. Since the building width is the only variable in Eq. (19), the equation can be simplified as what is shown in Eq. (20), where the B_l stands for the building length, which varies from 5 to 15 meters.

$$A_{ls}/A_g = \frac{Fl_A + 2\times Fc_A + R_A}{2\times Fl_A + A_{UA}} \tag{19}$$

$$A_{ls}/A_g = \frac{5B_l + 54 + 10\sqrt{\frac{B_l^2}{2}} + 5.76}{11.875B_l} \tag{20}$$

The mentioned settings lead to the approximate range of variability for A_{ls}/A_g between 1.91 to 1.15.

9.2 Determining the minimum enough simulations for a robust result

First, for determining enough simulations to reach the convergence in both Morris and Sobol methods, ranking parameter comparison with an increasing trajectory approach was applied. For the Morris method, the simulation started with 40 and ended with 10240 trajectories with doubling the trajectories' size in each step (Figure 14). For the Sobol method, since it inherently needs many more number simulations than other SA methods, the coefficient value started ten times greater than the Morris method with 400 and stopped at 102400 (Figure 15). The number of simulations in each step is equal to $n(k+1)$ and $2n(k+1)$ for Morris and Sobol method respectively, where k is the number of input parameters, which here is equal to 17 based on Table 5, and n is the number of trajectories for Morris's method and coefficient value for the Sobol's method.

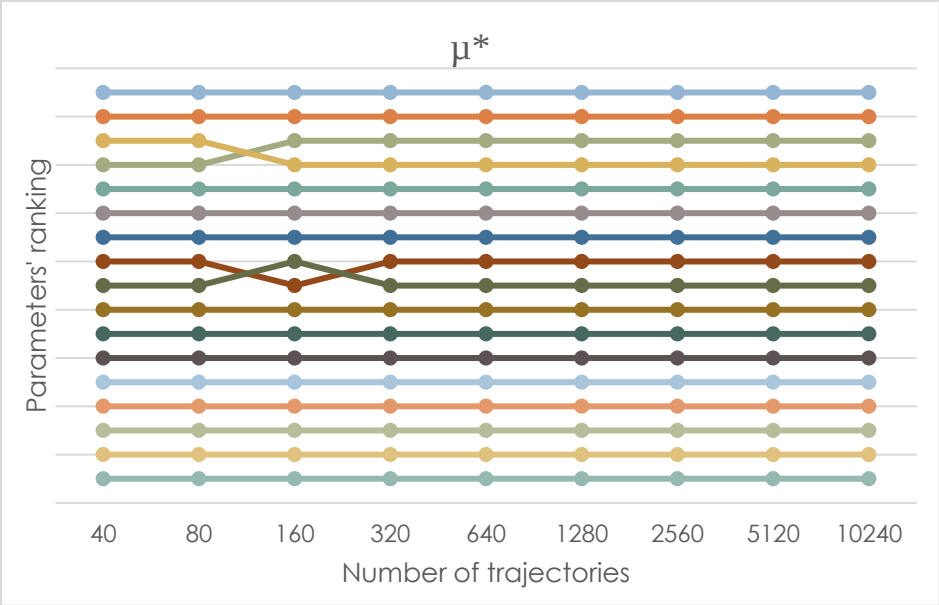

Figure 14- Relative ranking of input parameters for the given trajectory number based on μ value in the Morris method*

Figure 14 shows how parameters' ranking change with doubling the number of trajectories for the Morris method. According to Figure 14, for our model with the mentioned input factors, choosing a trajectory number greater than 320 can lead to robust results in ranking all Morris method factors. For the Sobol method, the total-order sensitivity measure, S_T, is used for determining negligible parameters, and the first-order sensitivity measure, S_1, for determining the most influential parameters.

As seen in Figure 14, the relative rankings of input factors based on the measure S_T are consistent with the coefficient value of 6400. Still, their ranks based on S_1 keeps fluctuating even in higher numbers. This phenomenon shows that reaching the full convergence of the Sobol method requires numerous simulations, which is the reason for making it very computationally expensive. However, from Figure 15, it is evident that the ten most influential parameters are almost consistent in orders for the coefficient values higher than 6400, and flections are related to the least important parameters whose S_T is the measure of order, not S_1.

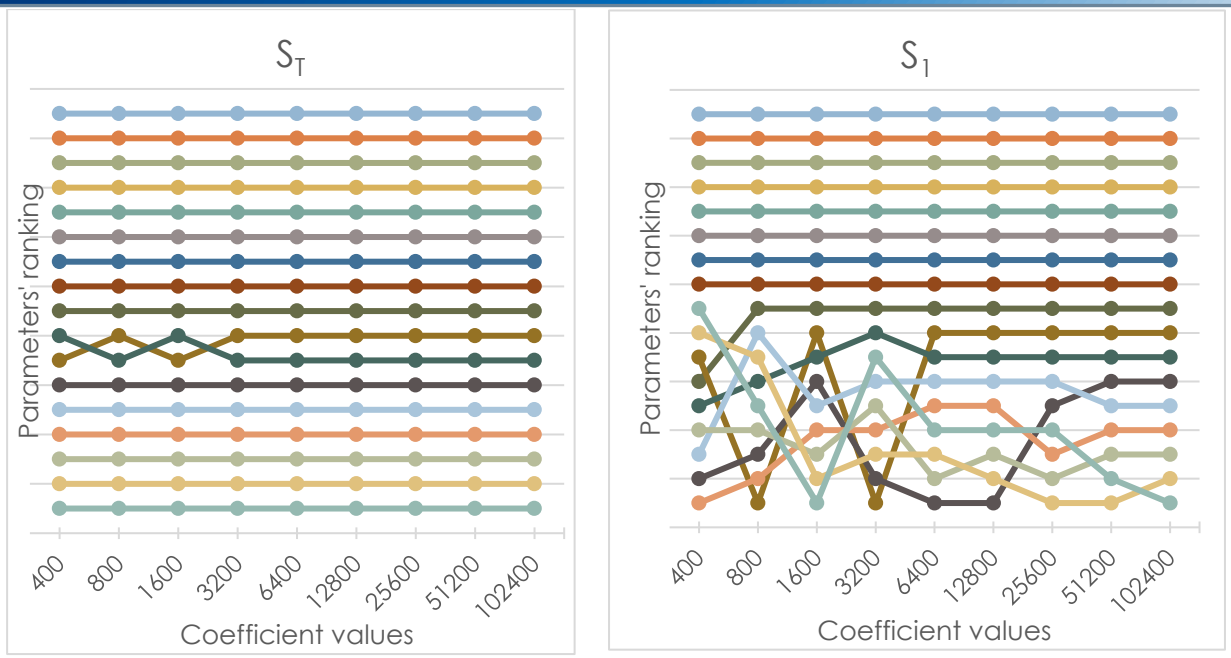

Figure 15- Left: relative ranking of input parameters for the given coefficient number based on S_t value in the Sobol method, right: relative ranking of input parameters for the given coefficient number based on St value in the Sobol method

9.3 Sensitivity analyses settings

The sensitivity analyses were conducted for the BENG1 value as a scaler output of the model. The BENG1 value is an indicator of the total heating and cooling energy requirement, which is calculated in kWh/m^2 per year. For Morris's method, the number of levels and trajectories were set on 14 and 10240, respectively, which resulted in 163840 simulations. Also, Sobol's coefficient value was considered 102400, leading to a total of 3,481,600 simulations for Sobol sensitivity analysis.

10. Results and discussion

10.1 SA ranking results

Tables 6 summarizes both Sobol and Morris methods' sensitivity measures resulting from sensitivity analyses for the model output, BENG1 value.

Table 6- Sensitivity measures of the input factors considering BENG1 as the model's target output

Parameters ranked by S_T	Sobol's measures		Morris's measures	
	S_1	S_T	μ^*	σ
Als/Ag	0.3403	0.3871	46.7482	27.0216
Window to Wall Ratio	0.1941	0.2522	36.8152	22.0452
Window U	0.1639	0.2053	34.1940	18.3421
Infiltration Rate	0.1049	0.1056	27.2538	2.4074
Facades Rc	0.0412	0.0456	15.1574	13.8789
Roof Rc	0.0361	0.0367	13.9962	11.7750
Floor Rc	0.0205	0.0210	11.0565	5.7789
Specific Internal Heat Capacity	0.0106	0.0190	8.0246	11.1094
Window Obstruction	0.0055	0.0087	5.5338	5.0508
Window G	0.0026	0.0057	4.5009	6.5799
Orientation	0.0009	0.0020	2.4855	3.6835
Sunblind Type	0.0001	0.0020	2.3379	3.5110
Frame Fraction	0.0002	0.0008	1.9550	2.1167
Sunblind Colour	0.0000	0.0002	0.4220	1.0354
Sunblind Control	0.0000	0.0000	0.0000	0.0000

Based on the Sobol method's sensitivity indices, factors with sensitivity either first-order or total-order index value greater than 0.05 can be considered influential on the output variations. From Tables 6 and 7, "Als/Ag", "Window to wall ratio", "Window U", "Infiltration Rate"," Facade Rc", and "Roof Rc" for both model's output have Sobol indices more than 0.05. Figure 16 visualizes the Sobol indices values of input factors and their relative influence ranking based on total-order sensitivity indices.

As mentioned earlier in section 8.1, the Morris method resulted in qualitative results. The notions of influential and non-influential parameters are based on the relative locations of elementary effects' statistics in the plane. Typically, the non-influential ones are clustered closer to the origin (relative to the more influential ones) with a pronounced boundary. Figure 17 represents the μ*-σ chart from the Morris method. The area within the red cycles in the figure represents negligible parameters, while the green circle represents the influential ones. As can be seen, the detected influential parameters in both SA methods for each model's output are the same, which indicates the robustness of the conducted sensitivity analyses.

Moreover, from the μ*-σ chart, it can be inferred that roof and façade R-values have almost nonlinear effects on the output results since they are close to the σ/μ^* = 1 line. On the other hand, changes in infiltration rate demonstrate a highly linear behavior towards changes in the BENG1 value.

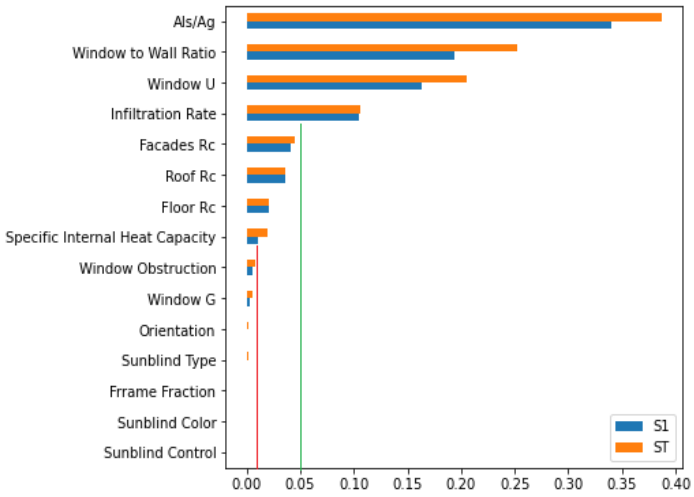

Figure 16 - Sobol indices measures of input parameters for BENG1 value ranked by total sensitivity measures

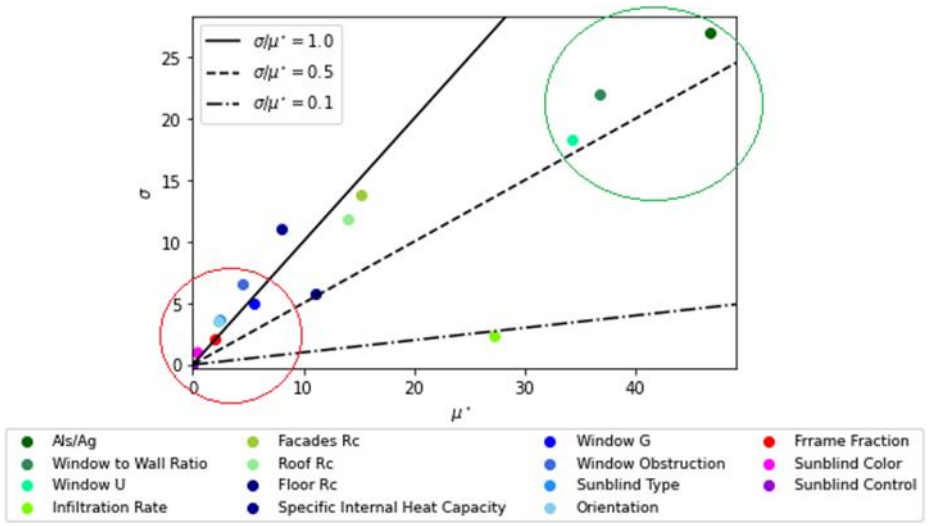

Figure 17 – The μ-σ chart result of the Morris method. Red circle: The parameters with negligible effects*

10.2 Discussion

Figures 18 to 20 show the changes in the BENG1 based on the changes in each influential parameter identified from sensitivity analysis. The charts' values have been extracted from Sobol analysis. Each point on the graphs below represents a single simulation in which the x-axis value equals the amount of change in the specific parameter, and the y-axis represents the change in the target output derived from the change in that input. Moreover, each graph contains information regarding the linear regression between the input parameters' changes and the relative target output change.

As it previously turned out from the Morris SA result, here also can be seen the highly linear ($R^2 = 0.98$) relationship between changes in BENG1 and changes in the and infiltration rate values. Figures 18 to 20 also show that the absolute range of changes in the target outputs derived from changes within each input factor's range has a significant role in determining its sensitivity indices values in the Sobol method. For instance, Als/Ag and window to wall ratio, ranked as the first and second most influential parameters, cover the approximate range of -100 to 100 and -80 to 80 respectively of the

changes in the BENG1 value, which is higher than the variation ranges result from all other input parameters.

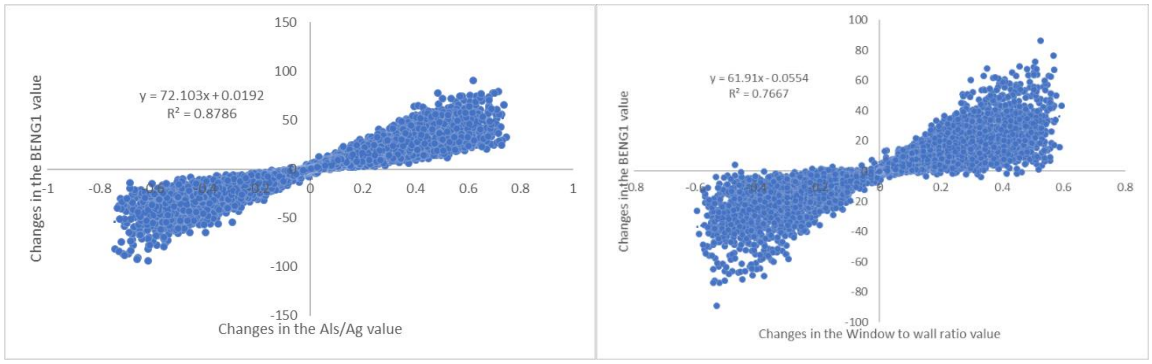

Figure 18- Changes in the BENG1 value from changes in the value of Als/Ag (left) and window to wall ratio (right)

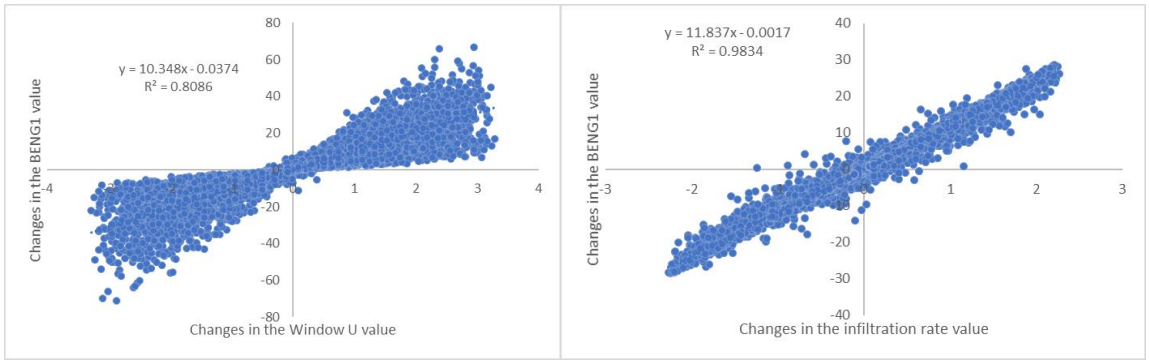

Figure 19 - Changes in the BENG1 value from changes in the value of Window U (left) and infiltration rate (right)

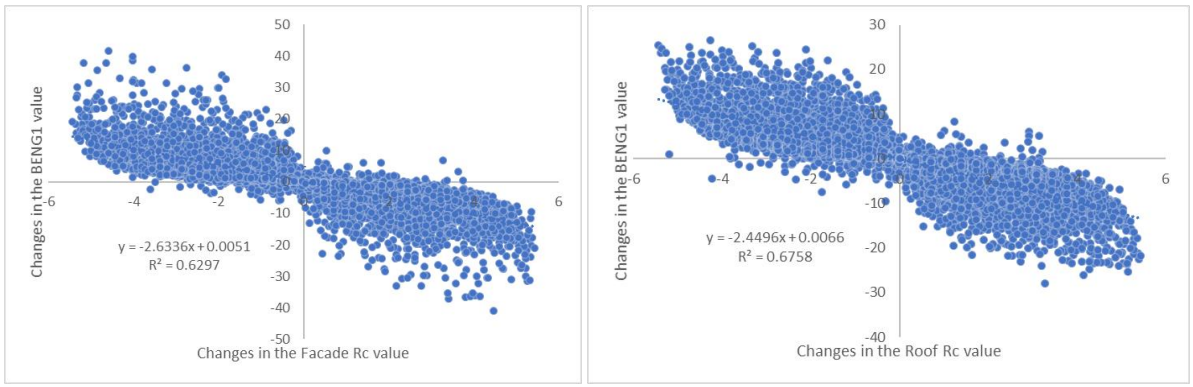

Figure 20- Changes in the BENG1 value from changes in the value of Façade Rc (left) and Roof Rc (right)

From an in-depth analysis of the Morris method results, it was found that insulation properties' parameters have a highly non-linear behavior, which means a constant change within their variability range from different start point leads to very different variation ranges for the BENG1 value. Figure 22 and Table 7 show that when R values are close to their lowest boundary, a fixed increment in their value influences the BENG1 variation much more than when they are in the middle or close to the upper bound of their variability range.

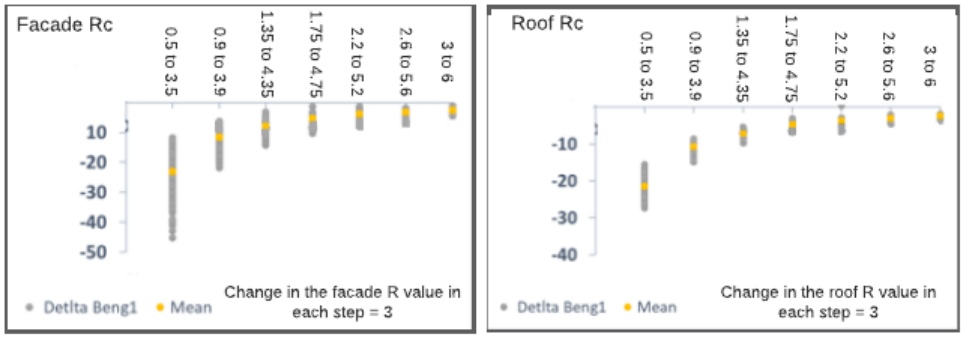

Figure 21 - The variation range and their mean values of BENG1 for each step number of Façade Rc (left) and Roof Rc (right)

Table 7 - Variation details for each step number in input and output values for Roof Rc and Façade Rc

Step Number	Facade Rc		BENG1		Roof Rc		BENG1	
	Input variations		Output variations		Input variations		Output variations	
	From	To	Range	Mean	From	To	Range	Mean
1	0.5	3.5	28.78	-22.85	0.5	3.5	28.78	-21.71
2	0.9	3.9	16.54	-9.03	0.9	3.9	16.54	-11.10
3	1.35	4.35	16.44	-7.10	1.35	4.35	16.44	-7.23
4	1.75	4.75	10.87	-6.13	1.75	4.75	10.87	-5.2
5	2.2	5.2	10.95	-5.84	2.2	5.2	10.95	-3.34
6	2.6	5.2	7.76	-3.88	2.6	5.2	7.76	-2.17
7	3	6.00	6.29	-2.85	3	6.00	6.29	-1.76

11. Conclusion

Determining the current state of dwellings' energy performance as well as the ability to generate suitable renovation solutions based on their current state is necessary for accelerating the mass-scale renovation rate. In this regard, providing useable information would be crucial for proper simulation and analysis. However, seeking all the required data simultaneously and making them useable require a massive effort, which in some cases, might be infeasible to fulfil. Thus, prioritizing input information is essential to facilitate and illuminate the orderly way of acquiring preliminary information. This report's conducted study tried to ascertain the prioritization of the most and least influential parameters for determining the total heating and cooling energy demand (BENG1) derived from NTA8800 regulations. Thus, two well-known global sensitivity analysis methods, commonly used in the building energy performance simulations (Morris's and Sobol's methods), were selected to apply on the WoonConnect energy calculation software. Based on the literature, fifteen physical characteristics of a typical three-floor row dwelling were chosen as the analyses' input factors. The analyses were performed with an adequate number of simulations to ensure results' robustness, which was further confirmed by attaining the same results from both applied methods. From what previously discussed, the input factors can be categorized into three priority levels.

Priority Level 1: the parameters with the first and total sensitivity measures greater than 0.05 (S_1, S_T > 0.05). These parameters are highly influential, so that even small changes in each may significantly impact in determining the BENG1 value. This category includes "Compactness (Als/Ag)", "Window to wall ratio", "Window U", and the "Infiltration rate". The first two parameters are directly derived from dwelling geometrical characteristics, and the others depend on glazing and construction year, respectively.

Priority Level 2: the parameters with the first and total sensitivity measures between 0.01 to 0.05 (0.01< S_1, S_T < 0.05). These parameters are not as influential as the ones in the first category, which means that their variation would not significantly impact the value of BENG1. This category consists of façade, roof, floor R values, and specific internal heat capacity. For determining R values, material and insulation of dwellings must be considered and the value of specific internal heat capacity specified based on the construction mass, which must also be calculated based on the building's structural material weight. Although this category's parameters are not as influential as those in the first one, the uncertainty for determining them should be minimized as much as possible since their non-linear behavior makes them more influential as their value approaches the lower limits (e.g., R values less than one).

Priority Level 3: the parameters with the first and total sensitivity measures less than 0.01 (S1, ST < 0.01). As the sensitivity measures approach zero, the parameters' changes do not lead to a significant range of variations in the output value compared to the other input factors. Moreover, in contrast to the highly influential parameters, there are no distinct patterns between the changes in the value of the parameters in this category and the subsequent variation in the value of BENG1. This category encompasses seven parameters mostly related to the sun radiation, namely window obstruction, G value, orientation, frame fraction, and sunblind settings.

Table 8 summarized the input parameters' categorization based on sensitivity measures. Note that this categorization is only valid for the parameters considered as input factors in this study, and it is limited

to the analyses on the BENG1 value. So, the prioritization and parameters influence might differ, considering other target outputs such as primary energy consumption or users' comfort. Due to the NTA8800 requirements, this study is limited in terms of the number of influential parameters for determining dwellings' heating and cooling energy demand. The NTA8800 has been developed to assess houses for energy efficiency. This standard is based on average use and average conditions (for the Netherlands). This was done to be able to compare dwellings with each other in the most objective way possible. It is therefore impossible to make a correct prediction with the NTA8800 of the actual energy demand of a house and its residents without taking into account the regional differences in climate, heat flows between rooms and residents' behavior.

Table 8 - Input parameters' categorization based on sensitivity measures range

Priority level	Sensitivity measure	Parameters	Change pattern	Source of information	Acceptable uncertainty
1	Greater than 0.05	Als/Ag	Linear	Geometrical properties	As exact as possible
		Window to Wall Ratio			
		Window U		Glazing	
		Infiltration Rate		Construction year	
2	Between 0.01 and 0.05	Facades Rc	non-linear	Thermal properties	Uncertainty should be minimized as values approach to the lower limits
		Roof Rc			
		Floor Rc			
		Specific Internal Heat Capacity	Almost linear	Construction mass	
3	Less than 0.001	Window Obstruction	no distinct pattern	Sun radiation	Better to be known if the information is available
		Window G			
		Orientation			
		Sunblind Type			
		Frame Fraction			
		Sunblind Colour			
		Sunblind Control			

From what has been achieved in this study, the project will be focused on gathering the required information based on their priority. In the next step, we will be focused on determining dwellings' geometrical properties from available data sources. One of the most valuable sources to obtain required geometrical information would be publicly available point clouds of existing dwellings, derived from aerial LiDAR surveys. Being available countrywide makes the point cloud a worthwhile data source from which useable information can be extracted to accelerate dwellings' energy demand calculations on large scales and subsequently facilitate the upscaling renovation process12.

12. Acknowledgements

This work is supported by the Topsector Energie grant and MMIP 3/4 grant from the Netherlands Ministry of Economic Affairs & Climate Policy as well as the Ministry of the Interior and Kingdom Relations.

13. References

[1] M. Aldanondo, A. Barco-Santa, E. Vareilles, P. Gaborit, M. Falcon, and L. Zhang, "Towards a BIM approach for a high performance renovation of apartment buildings," *IFIP Adv. Inf. Commun. Technol.*, vol. 442, pp. 21–30, 2014, doi: 10.1007/978-3-662-45937-9_3.

[2] O. Guerra-Santin *et al.*, "Considering user profiles and occupants' behaviour on a zero energy renovation strategy for multi-family housing in the Netherlands," *Energy Effic.*, vol. 11, no. 7, pp. 1847–1870, 2018, doi: 10.1007/s12053-018-9626-8.

[3] European Commission, "In focus: Energy Efficiency in Buildings," *European Commission website*, 2020. https://ec.europa.eu/info/news/focus-energy-efficiency-buildings-2020-feb-17_it.

[4] Eurostat, "Energy consumption and use by households - Product - Eurostat," 2019. https://ec.europa.eu/eurostat/en/web/products-eurostat-news/-/DDN-20190620-1 (accessed Oct. 07, 2020).

[5] M. Vavallo *et al.*, "Accelerating Energy Renovation Solution for Zero Energy Buildings and Neighbourhoods—The Experience of the RenoZEB Project," *Proceedings*, vol. 20, no. 1, p. 1, 2019, doi: 10.3390/proceedings2019020001.

[6] A. GÖKGÜR and GÖKGÜR, A., "Current and future use of BIM in renovation projects," *Chalmers, Univ. Technol.*, p. 32, 2015.

[7] S. Ebrahimigharehbaghi, Q. K. Qian, F. M. Meijer, and H. J. Visscher, "Unravelling Dutch homeowners' behaviour towards energy efficiency renovations: What drives and hinders their decision-making?," *Energy Policy*, vol. 129, no. February, pp. 546–561, 2019, doi: 10.1016/j.enpol.2019.02.046.

[8] Official Journal of the European Union, "Directive 2012/27/EU of the European Parliament and of the Council of 25 October 2012 on Energy Efficiency, Amending Directives 2009/125/EC and 2010/30/EU and Repealing Directives 2004/8/EC and 2006/32/EC," *Official Journal of the European Union*, 2012.

[9] N. H. Sandberg *et al.*, "Dynamic building stock modelling: Application to 11 European countries to support the energy efficiency and retrofit ambitions of the EU," *Energy Build.*, vol. 132, pp. 26–38, 2016, doi: 10.1016/j.enbuild.2016.05.100.

[10] S. Ebrahimigharehbaghi, F. Filippidou, P. Van Den Brom, Q. K. Qian, and H. J. Visscher, "Analysing the energy efficiency renovation rates in the Dutch residential sector," *E3S Web Conf.*, vol. 111, no. 201 9, 2019, doi: 10.1051/e3sconf/201911103019.

[11] 2019 Haines et al, A. goleman, daniel; boyatzis, Richard; Mckee, 2019 Haines et al, A. goleman, daniel; boyatzis, Richard; Mckee, 2019 Haines et al, and A. goleman, daniel; boyatzis, Richard; Mckee, "A Renovation Wave for Europe," *J. Chem. Inf. Model.*, vol. 53, no. 9, pp. 1689–1699, 2019.

[12] A. Saltelli, S. Tarantola, F. Campolongo, and M. Ratto, *Sensitivity analysis in practice: a guide to assessing scientific models (Google eBook)*. 2004.

[13] L. G. M. Gorris and C. Yoe, *Risk Analysis: Risk Assessment: Principles, Methods, and*

Applications, vol. 1. Elsevier Ltd., 2014.

[14] C. Pichery, *Sensitivity Analysis*, Third Edit., vol. 3. Elsevier, 2014.

[15] S. Hoops *et al.*, *Ordinary Differential Equations (ODEs) Based Modeling*. Elsevier Inc., 2016.

[16] DJ Pannell, "Sensitivity analysis of normative economic models: theoretical framework and practical strategies," *Agric. Econ.*, vol. 16, pp. 139–152, 1997, [Online]. Available: http://www.sciencedirect.com/science/article/pii/S0169515096012170.

[17] T. Wei, "A review of sensitivity analysis methods in building energy analysis," *Renew. Sustain. Energy Rev.*, vol. 20, pp. 411–419, 2013, doi: 10.1016/j.rser.2012.12.014.

[18] Z. Pang, Z. O'Neill, Y. Li, and F. Niu, "The role of sensitivity analysis in the building performance analysis: A critical review," *Energy and Buildings*, vol. 209. Elsevier B.V., p. 109659, 2020, doi: 10.1016/j.enbuild.2019.109659.

[19] G. M. Mauro, M. Hamdy, G. P. Vanoli, N. Bianco, and J. L. M. Hensen, "A new methodology for investigating the cost-optimality of energy retrofitting a building category," *Energy Build.*, vol. 107, pp. 456–478, 2015, doi: 10.1016/j.enbuild.2015.08.044.

[20] F. Ascione, N. Bianco, C. De Stasio, G. M. Mauro, and G. P. Vanoli, "Artificial neural networks to predict energy performance and retrofit scenarios for any member of a building category: A novel approach," *Energy*, vol. 118, pp. 999–1017, 2017, doi: 10.1016/j.energy.2016.10.126.

[21] S. Yang, W. Tian, E. Cubi, Q. Meng, Y. Liu, and L. Wei, "Comparison of Sensitivity Analysis Methods in Building Energy Assessment," in *Procedia Engineering*, 2016, vol. 146, pp. 174–181, doi: 10.1016/j.proeng.2016.06.369.

[22] X. Chen, H. Yang, and W. Zhang, "A comprehensive sensitivity study of major passive design parameters for the public rental housing development in Hong Kong," *Energy*, vol. 93, pp. 1804–1818, 2015, doi: 10.1016/j.energy.2015.10.061.

[23] S. Gou, V. M. Nik, J. L. Scartezzini, Q. Zhao, and Z. Li, "Passive design optimization of newly-built residential buildings in Shanghai for improving indoor thermal comfort while reducing building energy demand," *Energy Build.*, vol. 169, pp. 484–506, 2018, doi: 10.1016/j.enbuild.2017.09.095.

[24] N. Delgarm, B. Sajadi, K. Azarbad, and S. Delgarm, "Sensitivity analysis of building energy performance: A simulation-based approach using OFAT and variance-based sensitivity analysis methods," *J. Build. Eng.*, vol. 15, no. July 2017, pp. 181–193, 2018, doi: 10.1016/j.jobe.2017.11.020.

[25] J. Egan *et al.*, "Definition of a useful minimal-set of accurately-specified input data for Building Energy Performance Simulation," *Energy Build.*, vol. 165, pp. 172–183, 2018, doi: 10.1016/j.enbuild.2018.01.012.

[26] Y. Sun, "Sensitivity analysis of macro-parameters in the system design of net zero energy building," *Energy Build.*, vol. 86, pp. 464–477, 2015, doi: 10.1016/j.enbuild.2014.10.031.

[27] M. Ferrara, E. Sirombo, A. Monti, E. Fabrizio, and M. Filippi, "Influence of Envelope Design in the Optimization of the Energy Performance of a Multi-family Building," in *Energy Procedia*, 2017, vol. 111, no. September 2016, pp. 308–317, doi: 10.1016/j.egypro.2017.03.095.

[28] M. H. Abokersh, M. Spiekman, O. Vijlbrief, T. A. J. van Goch, M. Vallès, and D. Boer, "A real-

time diagnostic tool for evaluating the thermal performance of nearly zero energy buildings," *Appl. Energy*, vol. 281, no. October 2020, 2021, doi: 10.1016/j.apenergy.2020.116091.

[29] M. Mosteiro-Romero, J. A. Fonseca, and A. Schlueter, "Seasonal effects of input parameters in urban-scale building energy simulation," in *Energy Procedia*, 2017, vol. 122, pp. 433–438, doi: 10.1016/j.egypro.2017.07.459.

[30] W. Tian *et al.*, "Building Energy Assessment Based on a Sequential Sensitivity Analysis Approach," in *Procedia Engineering*, 2017, vol. 205, pp. 1042–1048, doi: 10.1016/j.proeng.2017.10.168.

[31] T. Yang, Y. Pan, J. Mao, Y. Wang, and Z. Huang, "An automated optimization method for calibrating building energy simulation models with measured data: Orientation and a case study," *Appl. Energy*, vol. 179, pp. 1220–1231, 2016, doi: 10.1016/j.apenergy.2016.07.084.

[32] A. S. Silva, L. S. S. Almeida, and E. Ghisi, "Decision-making process for improving thermal and energy performance of residential buildings: A case study of constructive systems in Brazil," *Energy Build.*, vol. 128, pp. 270–286, 2016, doi: 10.1016/j.enbuild.2016.06.084.

[33] F. Bre, A. S. Silva, E. Ghisi, and V. D. Fachinotti, "Residential building design optimisation using sensitivity analysis and genetic algorithm," *Energy Build.*, vol. 133, pp. 853–866, 2016, doi: 10.1016/j.enbuild.2016.10.025.

[34] S. Liu, Y. T. Kwok, K. K. L. Lau, W. Ouyang, and E. Ng, "Effectiveness of passive design strategies in responding to future climate change for residential buildings in hot and humid Hong Kong," *Energy Build.*, vol. 228, p. 110469, 2020, doi: 10.1016/j.enbuild.2020.110469.

[35] C. Zhu, W. Tian, B. Yin, Z. Li, and J. Shi, "Uncertainty calibration of building energy models by combining approximate Bayesian computation and machine learning algorithms," *Appl. Energy*, vol. 268, no. September 2019, p. 115025, 2020, doi: 10.1016/j.apenergy.2020.115025.

[36] T. C. Lam, H. Ge, and P. Fazio, "Impact of curtain wall configurations on building energy performance in the perimeter zone for a cold climate," in *Energy Procedia*, 2015, vol. 78, pp. 352–357, doi: 10.1016/j.egypro.2015.11.665.

[37] S. Li, K. Deng, and M. C. Zhou, "Sensitivity Analysis for Building Energy Simulation Model Calibration via Algorithmic Differentiation," *IEEE Trans. Autom. Sci. Eng.*, vol. 14, no. 2, pp. 905–914, 2017, doi: 10.1109/TASE.2016.2573821.

[38] A. Prada, G. Pernigotto, P. Baggio, and A. Gasparella, "Uncertainty propagation of material properties in energy simulation of existing residential buildings: The role of buildings features," *Build. Simul.*, vol. 11, no. 3, pp. 449–464, 2018, doi: 10.1007/s12273-017-0418-4.

[39] L. La Fleur, P. Rohdin, and B. Moshfegh, "Investigating cost-optimal energy renovation of a multifamily building in Sweden," *Energy Build.*, vol. 203, 2019, doi: 10.1016/j.enbuild.2019.109438.

[40] J. D. Herman, J. B. Kollat, P. M. Reed, and T. Wagener, "Technical note: Method of Morris effectively reduces the computational demands of global sensitivity analysis for distributed watershed models," *Hydrol. Earth Syst. Sci. Discuss.*, vol. 10, no. 4, pp. 4275–4299, Apr. 2013, doi: 10.5194/hessd-10-4275-2013.

[41] E. de Rocquigny, N. Devictor, and S. Tarantola, Eds., *Uncertainty in Industrial Practice*. Chichester, UK: John Wiley & Sons, Ltd, 2008.

[42] F. Pianosi *et al.*, “Sensitivity analysis of environmental models: A systematic review with practical workflow,” *Environmental Modelling and Software*, vol. 79. Elsevier Ltd, pp. 214–232, 2016, doi: 10.1016/j.envsoft.2016.02.008.

[43] M. D. Morris, “Factorial Sampling Plans for Preliminary Computational Experiments,” *Technometrics*, vol. 33, no. 2, p. 161, May 1991, doi: 10.2307/1269043.

[44] G. Pujol and G. Pujol, “Simplex-based screening designs for estimating metamodels To cite this version : HAL Id : hal-00305313 Simplex-based screening designs for estimating metamodels,” 2009.

[45] F. Campolongo, J. Cariboni, and A. Saltelli, “An effective screening design for sensitivity analysis of large models,” vol. 22, 2007, doi: 10.1016/j.envsoft.2006.10.004.

[46] F. Campolongo, J. Cariboni, and A. Saltelli, “An effective screening design for sensitivity analysis of large models,” *Environ. Model. Softw.*, vol. 22, no. 10, pp. 1509–1518, 2007, doi: 10.1016/j.envsoft.2006.10.004.

[47] K. Menberg, Y. Heo, and R. Choudhary, “Sensitivity analysis methods for building energy models : Comparing computational costs and extractable information,” vol. 133, pp. 433–445, 2016.

[48] I. M. Sobol, “Global sensitivity indices for nonlinear mathematical models and their Monte Carlo estimates,” *Math. Comput. Simul.*, vol. 55, no. 1–3, pp. 271–280, 2001, doi: 10.1016/S0378-4754(00)00270-6.

[49] A. Saltelli, P. Annoni, I. Azzini, F. Campolongo, M. Ratto, and S. Tarantola, “Variance based sensitivity analysis of model output . Design and estimator for the total sensitivity index,” *Comput. Phys. Commun.*, vol. 181, no. 2, pp. 259–270, 2010, doi: 10.1016/j.cpc.2009.09.018.

[50] B. Iooss and P. Lemaître, “A Review on Global Sensitivity Analysis Methods,” in *Operations Research/ Computer Science Interfaces Series*, vol. 59, G. Dellino and C. Meloni, Eds. Boston, MA: Springer US, 2015, pp. 101–122.

[51] A. Saltelli and T. Homma, “Importance measures in global sensitivity analysis of model output,” *Reliab. Eng. Sys. Saf.*, vol. 52, pp. 1–17, 1996.

[52] J. Herman and W. Usher, “SALib : Sensitivity Analysis Library in Python (Numpy). Contains Sobol , SALib : An open-source Python library for Sensitivity Analysis,” vol. 41, no. April, pp. 2015–2017, 2018, doi: 10.1016/S0010-1.